

CsSmGeS₄: A Novel Layered Mixed-Metal Sulfide Crystallizing in the Noncentrosymmetric Space Group *P*2₁2₁

Cordelia K. Bucher and Shiou-Jyh Hwu*

Department of Chemistry, Rice University, P. O. Box 1892, Houston, Texas 77251

Received June 29, 1994[Ⓞ]

A novel mixed-metal sulfide compound CsSmGeS₄ was isolated from a reaction intended to grow single crystals of AgSm₃GeS₇ via the CsCl molten flux. The title compound possesses an unusual structural feature, a helix made of CsS₈ units, which is likely responsible for the formation of the noncentrosymmetric lattice. This compound crystallizes in an orthorhombic unit cell with $a = 6.768$ (2) Å, $b = 17.752$ (2) Å, $c = 6.488$ (1) Å, $V = 779.5$ (3) Å³; *P*2₁2₁ (No. 19); $Z = 4$. The structural and thermal parameters were refined by full-matrix least-squares methods to $R = 0.057$, $R_w = 0.071$ and GOF = 2.18 based on F with 64 variables. The structure of this quaternary chalcogenide can be considered as a layered type in that the [SmGeS₄][−] slabs are stacked along the crystallographic b axis with cesium cations in the van der Waals gap between sulfur layers. The coordination of the CsS₈ unit is characterized by a planar pentagonal arrangement of sulfurs at a slight angle to the ab plane, with the three other sulfurs in the coordination sphere above the plane in a staggered orientation. The CsS₈ polyhedra are interconnected about a 2₁ screw axis to form a helix along the c direction. The differential thermal analysis (DTA) and preliminary infrared absorption spectroscopy studies suggest that the CsSmGeS₄ compound melts congruently at ~1086 °C and is likely IR transparent, respectively. The comparison of the title compound with the structurally related chalcogenides KLaGeS₄ (*P*2₁) and CaYbInS₄ (*Pnma*) is discussed.

Introduction

Non-metallic heavy-metal chalcogenide compounds are attractive because of their potential applications in an extended infrared transparency region.^{1–4} During our systematic exploratory synthesis of new optical materials, a wealth of mixed-metal chalcogenide compounds that contain rare-earth (RE) cations have been isolated.^{3–5} A number of studies have exhibited compounds with enhanced thermal stability and formation of a large variety of structural frameworks because of the incorporation of rare-earth cations.⁴ These recent advances in exploratory synthesis are attributed to the success in single crystal growth of rare-earth-containing refractory chalcogenides that otherwise would only be prepared in polycrystalline form. Via the flux-growth method, sizable single crystals have become available for detailed analyses that have rendered an in-depth understanding of structural chemistry and its correlation with unusual properties. While single crystal growth using molten halide fluxes has proven fruitful, it is generally realized that occasional inclusion of cations and/or halide anions in compound formation is inevitable. Serendipitously, a novel layered mixed-metal sulfide, CsSmGeS₄, has been isolated from a reaction intended to grow single crystals of AgSm₃GeS₇⁶ employing a CsCl molten salt flux.

The new cesium samarium germanium sulfide, CsSmGeS₄, crystallizing in the acentric space group *P*2₁2₁, is of great interest with respect to the “materials engineering” for synthesizing noncentrosymmetric crystals that are potentially useful for the nonlinear optical (NLO) device applications.⁷ Although a number of extended solids adopting noncentrosymmetric space groups have been identified,⁸ a first step in selecting possible NLO materials, systematic investigation of noncentrosymmetric crystals has been lacking. In this paper, we present detailed structural analysis of the newly synthesized CsSmGeS₄ compound and comparison with the structurally related KLaGeS₄⁹ and CaYbInS₄ phases⁵ as a step toward understanding the parameters that govern the formation of noncentrosymmetric lattices. The bulk synthesis, thermal analysis, and infrared spectroscopy of the title compound are discussed.

Experimental Section

Synthesis. Pale yellow transparent crystals of the title compound were produced via a two step synthetic route. The CsCl salt was added as a flux to the pre-prepared AgSm₃GeS₇ mixture in a 10:1 (by weight) flux to charge ratio. The reaction was carried out in an evacuated, carbon-coated silica ampoule and heated for 7 days at ca. 750 °C followed by slow cooling. Detailed synthetic procedures are provided in the supplementary material. Crystals of the title compound (50% yield) were isolated from the flux by washing the reaction product with deionized water, using suction filtration method. The reaction byproducts were Sm₄S₃(Si₂O₇), according to single crystal X-ray structure analyses, and a structurally unidentified coral square gem which is analyzed as containing Ag, Sm, and S. The title compound seems stable in air, showing no signs of appreciable degradation in crystal quality over a period of months.

* Abstract published in *Advance ACS Abstracts*, November 1, 1994.

- (1) (a) *Infrared Technology Fundamentals*; Spiro, I. J., Schlessinger, M., Eds; Marcel Dekker, Inc.: New York and Basel, 1989. (b) Window and Dome Technologies and Materials I. Klocek, P., Ed. *Proc. SPIE* 1989, 1112, and references cited therein. (c) Window and Dome Technologies and Materials II. Klocek, P., Ed. *Proc. SPIE* 1990, 1326, and references cited therein. (d) Johnson, C. E.; Vanderah, T. A.; Bauch, C. G.; Harris, D. C. in *Ceramics and Inorganic Crystals for Optics, Electro-Optics, and Nonlinear Conversion*. *Proc. SPIE* 1988, 968, 41.
- (2) (a) Kipp, D. O.; Lowe-Ma, C. K.; Vanderah, T. A. *Chem. Mater.* 1990, 2, 506–11. (b) Lowe-Ma, C. K.; Kipp, D. O.; Vanderah, T. A. *J. Solid State Chem.* 1991, 92, 520–530.
- (3) (a) Carpenter, J. D.; Hwu, S.-J. *Acta Crystallogr.* 1992, C48, 1164–1168. (b) Carpenter, J. D.; Hwu, S.-J. *J. Solid State Chem.* 1992, 97, 332–339.
- (4) Carpenter, J. D., Ph.D. Dissertation, Rice University, 1993.
- (5) Carpenter, J. D.; Hwu, S.-J. *Chem. Mater.* 1992, 4, 1368–1372.

- (6) Hwu, S.-J.; Bucher, C. K.; Carpenter, J. D.; Taylor, S. P. *Inorg. Chem.*, submitted for publication.
- (7) *Materials for Nonlinear Optics*; Marder, S. R., Sohn, J. E., Stucky, G. D., Eds., ACS Symposium Series 455; American Chemical Society: Washington, DC, 1991.
- (8) *Pearson's Handbook of Crystallographic Data for Intermetallic Phases*, 2nd ed.; Villars, P., Calvert, L. D., Eds.; ASM International: Materials Park, OH, 1991.
- (9) Wu, P.; Ibers, J. A. *J. Solid State Chem.* 1993, 107, 347–355.

Table 1. Crystallographic Data^a for CsSmGeS₄

chem formula	CsSmGeS ₄	fw	484.14
a, Å	6.768 (2)	space group	P2 ₁ 2 ₁ 2 ₁ (No. 19)
b, Å	17.752 (2)	T, °C	22
c, Å	6.488 (1)	λ, Å	0.71069
V, Å ³	779.5 (3)	ρ _{calcd} , gcm ⁻³	4.12
Z	4	linear abs coeff, cm ⁻¹	168.0
R ^b	0.057		
R _w ^c	0.071		

^a The cell constants are refined in the orthorhombic crystal system using twenty-five reflections ($9.01^\circ \leq 2\theta \leq 26.17^\circ$). ^b $R = \sum[|F_o| - |F_c|]/\sum|F_o|$. ^c $R_w = [\sum w(|F_o| - |F_c|)^2/\sum w|F_o|^2]^{1/2}$.

Table 2. Positional and Equivalent Thermal Parameters for CsSmGeS₄

atom	x	y	z	B _{eq} , ^a Å ²
Cs	0.0072(3)	0.0316(1)	0.0016(3)	2.51(8)
Sm	0.4807(2)	0.22714(7)	0.7077(2)	0.90(4)
Ge	0.0157(4)	0.3348(1)	0.7909(4)	0.90(8)
S(1)	0.2465(9)	0.1536(5)	0.401(1)	1.2(3)
S(2)	0.0741(9)	0.2190(4)	0.894(1)	1.3(2)
S(3)	0.012(1)	0.4079(3)	0.058(1)	1.4(2)
S(4)	0.2551(8)	0.3539(4)	0.564(1)	1.1(3)

^a Isotropic equivalent thermal parameters defined as $B_{eq} = (8\pi^2/3)$ trace U.

The polycrystalline CsSmGeS₄ phase was synthesized from the stoichiometric reaction of corresponding elements in a fused silica tube. The reaction was slowly heated up from room temperature to 550 °C for 3 days followed by 750 °C and kept isotherm for six days with one grinding. The pale-greenish powder was subject to X-ray analysis at room temperature by the diffraction technique using a Phillips PW 1840 Diffractometer equipped with Cu Kα radiation and Ni filter. NIST (National Institute of Standards and Technology) silicon internal standard was mixed with the sample. The diffraction patterns obtained ($10^\circ \leq 2\theta \leq 60^\circ$) were indexed and refined by the least-squares program LATT.¹⁰ The refined cell constants with 17 indexed reflections are in good agreement with that from the single crystal indexing (see Table 1): $a = 6.775$ (3) Å, $b = 17.747$ (7) Å, $c = 6.493$ (4) Å, $V = 780.6$ (7) Å³.

X-ray Single Crystal Structure Determination. The structure was determined by the single crystal X-ray diffraction method. The summary of crystallographic data is listed in Table 1. A total of 1085 reflections ($2\theta_{max} = 55^\circ$) were collected (at room temperature) from two octants ($+h, \pm k, l$), of which 717 reflections with $I > 3\sigma(I)$ were used for the structure solution. The space group was determined unambiguously according to the presence of systematic absence, $h00$ ($h = \text{odd}$), $0k0$ ($k = \text{odd}$), $00l$ ($l = \text{odd}$). An absorption correction was applied based upon three azimuthal scans ($2\theta = 11.11^\circ, 19.67^\circ, 25.32^\circ$). Redundant data were collected for Friedel pair analysis, and the results determined the correct enantiomorph. The atomic coordinates were found by the PATTERSON method using the program SHELXS-86.¹¹ The structural and thermal parameters were refined by full-matrix least-squares methods to $R = 0.057$, $R_w = 0.071$ and $GOF = 2.18$ based on F with 64 variables, using the TEXSAN software package.¹² The final positional and isotropic thermal parameters are given in Table 2.

The chemical contents were confirmed afterwards by qualitative chemical analysis using a Cameca SX-50 electron microprobe with a SUN-4/330 based control and reduction system (fitted with a PGT IMAX energy dispersive analyzer with Be window and 155 eV Mn Kα) resolution.

Differential Thermal Analysis (DTA). The thermal analysis of the title compound was performed on a Du Pont 9900 Thermal Analysis

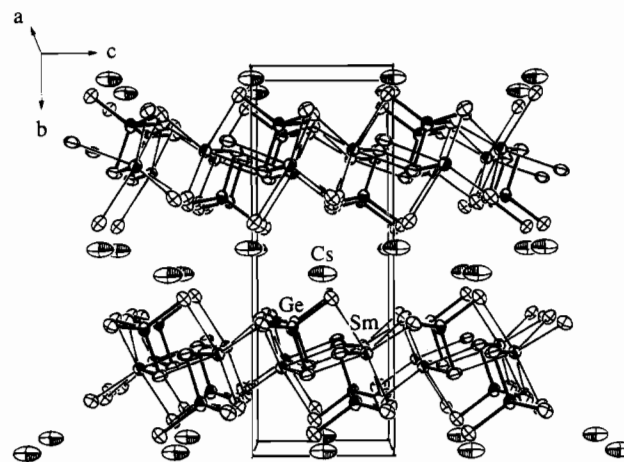


Figure 1. Unit cell of CsSmGeS₄ viewed along [100] of the orthorhombic lattice, as outlined. The anisotropic atoms are presented at 90% probability. The coordination of GeS₄ tetrahedra is drawn in thick bonds, and the SmS₇ monocapped trigonal prisms in thin bonds with the capping S to Sm bonds in double line.

System with using polycrystalline samples. The detailed experimental procedures are as similarly described in the previous report.⁵ A phase transition corresponding to congruent melting at ~ 1086 °C was observed. The sample changed color slightly from pale green to pale yellow presumably attributed to melting and consequently alternation of the phase morphology. The DTA product was examined by the X-ray diffraction method after the analysis to show consistent patterns.

Infrared Spectroscopy. Infrared spectra for polycrystalline samples were taken with a Perkin-Elmer 1600 series Spectrometer. Samples were pressed into pellets with KBr (Matheson, Reagent) powder. The obtained spectra ($4000\text{--}400$ cm⁻¹) showed only weak absorption bands due to water and carbon dioxide from the atmosphere similar to that of the previously reported CaYbInQ₄ (Q = S, Se) compounds.⁵ High-resolution single-crystal infrared transmittance spectroscopy later suggested that the CaYbInS₄ phase has a transparency cutoff at 10.3 μm.¹³

Results and Discussion

The CsSmGeS₄ phase crystallizes in an orthorhombic unit cell. In Figure 1, the ORTEP¹⁴ drawing shows the contents of the unit cell viewed along [100]. The germanium atom is coordinated to four sulfur atoms to form a Ge-centered GeS₄ tetrahedron, while the samarium atom coordinates with seven sulfur atoms to form a Sm-centered polyhedron which can be best described as a SmS₇ monocapped trigonal prism (mTP). The GeS₄ tetrahedra and SmS₇ mTPs share common edges to form extended [SmGeS₄]⁻ slabs within the ac plane of the unit cell. The GeS₄ and SmS₇ polyhedral geometries are commonly seen in a large collection of ternary and quaternary mixed-metal sulfides. The cesium atoms reside in the gap between the slabs. In viewing the orientation of each [SmGeS₄]⁻ slab, the capping sulfurs of the SmS₇ mTP are displaced in the same direction with respect to the bc plane, i.e., the corresponding Sm-S bonds (drawn in double lines) are pointing into the planes of the paper for the top slab of the unit cell and out of the plane for the bottom slab. These two slabs are symmetrically related by the 2₁ screw axes along [001] in the middle of the van der Waals gap at $x = 1/4$ and $3/4$.

The structure of the title compound can be considered as a layered type that is characterized by the [SmGeS₄]⁻ slabs with cesium cations residing in the van der Waals gaps. The layered

- (10) LATT: F. Takusagawa, Ames Laboratory, Iowa State University, Ames, Iowa, unpublished research, 1981.
 (11) Sheldrick, G. M. In *Crystallographic Computing 3*; Sheldrick, G. M., Krüger, C., Goddard, R., Eds.; Oxford University Press: London/New York, 1985; pp 175–189.
 (12) TEXSAN: Single Crystal Structure Analysis Software, version 5.0. Molecular Structure Corp., The Woodlands, TX, 1989.

- (13) Nadler, M. P.; Carpenter, J. D.; Hwu, S.-J. Unpublished research. Department of Chemistry, Rice University, Houston, TX, 1992.
 (14) Johnson, C. K. *ORTEP II*; Report ORNL-5138; Oak Ridge National Laboratory: Oak Ridge, TN, 1976.

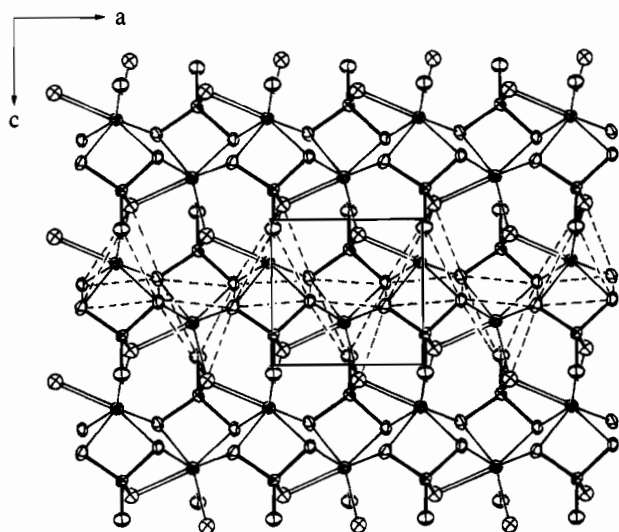


Figure 2. Structure of the extended $[\text{SmGeS}_4]^-$ slab shown along the ac plane (solid lines), with the coordination geometries drawn by three types of bonds noted in Figure 1. The middle row trigonal prisms of the SmS_7 mTPs are outlined (dotted lines) to depict the connectivity and the orientation. The anisotropic atoms are presented at 90% probability.

property is intuitively justified by the difference in the bonding nature of the largely covalent $[\text{SmGeS}_4]^-$ slabs vs primarily ionic layers of the Cs^+ cations. It is interesting to observe that a plate single crystal delaminates along the face that is consistent with the plane of the slabs upon applying mechanical pressure. When placed between two pieces of tape, a plate crystal splits into two pieces of the same morphology upon separation of the tape.

The extended $[\text{SmGeS}_4]^-$ slab structure is shown in Figure 2, where the coordination geometries are viewed approximately down onto the triangular planes of the SmS_7 mTPs. The middle row of trigonal prisms of the SmS_7 mTPs are outlined to show that the adjoining prisms share opposite edges of the square planes of the prism with apexes pointing alternately in opposite directions of c . This arrangement gives an extended sawtooth SmS_7 mTP chain with the edge-shared square planes slightly puckered. Two parallel mTP chains are interconnected by sharing "trans" edges of the GeS_4 units. The GeS_4 tetrahedron is arranged such that one of its sulfurs provides the seventh coordination, i.e., the capping sulfur, to an adjacent SmS_7 mTP.

The bond distances (Table 3) with respect to the GeS_4 and SmS_7 polyhedra are normal, and these polyhedral geometries are commonly seen. The Ge-S bond distances are reasonable, ranging from 2.17 Å to 2.22 Å, which are comparable with the sum of Shannon crystal radii, 2.23 Å, of four coordinated Ge^{4+} (0.53 Å) and S^{2-} (1.70 Å).¹⁵ The Sm-S bond distances are relatively diverse, in that the bond distances can be divided into two subsets. The Sm-S distances corresponding to the six apical sulfurs of the trigonal prism are shorter than the distance with respect to the single capping sulfur. The former distances are in the range of 2.83–2.94 Å while the later is 3.01 Å. The longer capping Sm-S distance is commonly seen and can be rationalized as "outersphere" coordination with respect to the samarium cation. In any case, the averaged Sm-S distance is 2.89 Å, which is consistent with the sum of the Shannon crystal radii, 2.86 Å, of seven coordinated Sm^{3+} (1.16 Å) and S^{2-} (1.70 Å).

The coordination geometry of the CsS_8 polyhedron, as shown in Figure 3, can be viewed as a pentagonal plane formed by

Table 3. Selected Bond Distances (Å) and Angles (deg) for CsSmGeS_4^a

SmS_7			
$\text{Sm-S}(1)^a$	2.860(8)	$\text{Sm-S}(1)^c$	2.867(7)
$\text{Sm-S}(2)^a$	3.010(6)	$\text{Sm-S}(2)^c$	2.825(7)
$\text{Sm-S}(3)^c$	2.846(6)	$\text{Sm-S}(4)^a$	2.874(7)
$\text{Sm-S}(4)^c$	2.936(7)		
$\text{S}(1)^a-\text{Sm-S}(1)^c$	120.9(1)	$\text{S}(1)^a-\text{Sm-S}(2)^a$	75.6(2)
$\text{S}(1)^a-\text{Sm-S}(2)^c$	156.1(2)	$\text{S}(1)^c-\text{Sm-S}(2)^a$	135.1(2)
$\text{S}(1)^c-\text{Sm-S}(2)^c$	80.5(2)	$\text{S}(1)^a-\text{Sm-S}(3)^c$	91.6(2)
$\text{S}(1)^c-\text{Sm-S}(3)^c$	135.0(2)	$\text{S}(1)^a-\text{Sm-S}(4)^a$	80.6(2)
$\text{S}(1)^c-\text{Sm-S}(4)^a$	71.1(2)	$\text{S}(1)^c-\text{Sm-S}(4)^c$	79.5(2)
$\text{S}(2)^a-\text{Sm-S}(2)^c$	81.6(1)	$\text{S}(2)^a-\text{Sm-S}(3)^c$	79.2(2)
$\text{S}(2)^c-\text{Sm-S}(3)^c$	77.3(2)	$\text{S}(2)^a-\text{Sm-S}(4)^a$	71.5(2)
$\text{S}(2)^c-\text{Sm-S}(4)^c$	142.8(2)	$\text{S}(2)^c-\text{Sm-S}(4)^a$	98.7(2)
$\text{S}(2)^c-\text{Sm-S}(4)^c$	124.9(2)	$\text{S}(3)^c-\text{Sm-S}(4)^a$	150.7(2)
$\text{S}(3)^c-\text{Sm-S}(4)^c$	82.0(2)	$\text{S}(4)^a-\text{Sm-S}(4)^c$	121.6(1)
GeS_4			
$\text{Ge-S}(1)^c$	2.216(7)	$\text{Ge-S}(2)^a$	2.199(7)
$\text{Ge-S}(3)^a$	2.167(7)	$\text{Ge-S}(4)^a$	2.216(7)
$\text{S}(1)^c-\text{Ge-S}(2)^a$	114.0(3)	$\text{S}(1)^c-\text{Ge-S}(3)^a$	112.6(3)
$\text{S}(1)^c-\text{Ge-S}(4)^a$	102.3(3)	$\text{S}(2)^a-\text{Ge-S}(3)^a$	108.5(3)
$\text{S}(2)^a-\text{Ge-S}(4)^a$	102.4(3)	$\text{S}(3)^a-\text{Ge-S}(4)^a$	116.7(3)
CsS_8			
$\text{Cs-S}(1)^a$	3.745(8)	$\text{Cs-S}(1)^b$	3.743(8)
$\text{Cs-S}(2)^a$	3.428(7)	$\text{Cs-S}(3)^a$	3.603(8)
$\text{Cs-S}(3)^c$	3.540(8)	$\text{Cs-S}(3)^d$	3.605(6)
$\text{Cs-S}(4)^c$	3.872(8)	$\text{Cs-S}(4)^d$	3.646(8)
$\text{S}(1)^a-\text{Cs-S}(1)^b$	115.8(2)	$\text{S}(1)^a-\text{Cs-S}(2)^a$	61.5(2)
$\text{S}(1)^a-\text{Cs-S}(3)^c$	59.5(1)	$\text{S}(1)^a-\text{Cs-S}(3)^e$	108.1(1)
$\text{S}(1)^a-\text{Cs-S}(3)^d$	79.6(2)	$\text{S}(1)^a-\text{Cs-S}(4)^a$	51.9(1)
$\text{S}(1)^a-\text{Cs-S}(4)^d$	142.3(2)	$\text{S}(1)^b-\text{Cs-S}(2)^a$	139.3(2)
$\text{S}(1)^b-\text{Cs-S}(3)^c$	79.7(1)	$\text{S}(1)^b-\text{Cs-S}(3)^e$	132.0(2)
$\text{S}(1)^b-\text{Cs-S}(3)^d$	67.6(2)	$\text{S}(1)^b-\text{Cs-S}(4)^c$	141.7(2)
$\text{S}(1)^b-\text{Cs-S}(4)^d$	55.7(1)	$\text{S}(2)^a-\text{Cs-S}(3)^c$	64.1(1)
$\text{S}(2)^a-\text{Cs-S}(3)^e$	79.0(1)	$\text{S}(2)^a-\text{Cs-S}(3)^d$	139.2(2)
$\text{S}(2)^a-\text{Cs-S}(4)^c$	72.3(2)	$\text{S}(2)^a-\text{Cs-S}(4)^d$	151.7(2)
$\text{S}(3)^c-\text{Cs-S}(3)^e$	142.7(2)	$\text{S}(3)^c-\text{Cs-S}(3)^d$	107.5(2)
$\text{S}(3)^c-\text{Cs-S}(4)^c$	109.9(1)	$\text{S}(3)^c-\text{Cs-S}(4)^d$	135.0(1)
$\text{S}(3)^c-\text{Cs-S}(3)^d$	103.7(2)	$\text{S}(3)^e-\text{Cs-S}(4)^c$	60.2(1)
$\text{S}(3)^e-\text{Cs-S}(4)^d$	77.8(1)	$\text{S}(3)^d-\text{Cs-S}(4)^c$	74.1(2)
$\text{S}(3)^d-\text{Cs-S}(4)^d$	63.1(2)	$\text{S}(4)^c-\text{Cs-S}(4)^d$	108.9(2)

^a Symmetry codes: (a) x, y, z ; (b) $x, y, 1 + z$; (c) $1/2 - x, -y, 1/2 + z$; (d) $1/2 - x, 1/2 + y, 1/2 + z$; (e) $-1/2 - x, -y, 1/2 + x$.

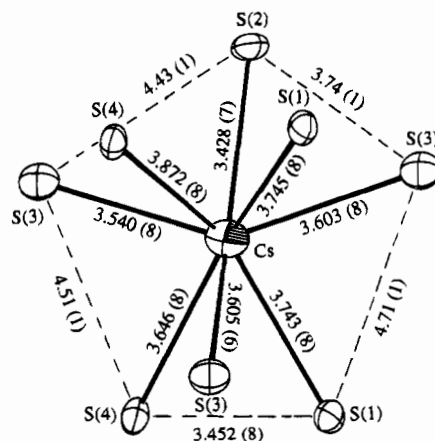


Figure 3. Coordination geometry of the CsS_8 unit viewed down onto the pentagonal plane of sulfurs. The bond distances are in ångströms.

five sulfur atoms with the other three sulfurs above the plane in a staggered orientation. Detailed structure analysis shows that the sum of the five S-Cs-S bond angles in the approximate pentagon is nearly circular, e.g., 356.24° , which suggests that the corresponding sulfurs are roughly co-planar. The pentagonal plane is at a slight angle to the ab plane with the three staggered

(15) Shannon, R. D. *Acta Crystallogr.* **1976**, *A32*, 751–67.

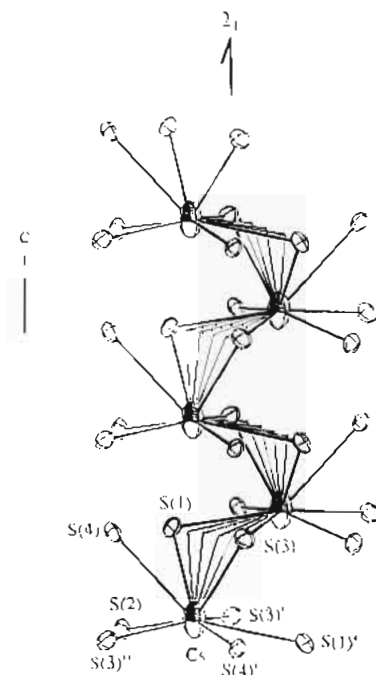


Figure 4. Helix made of CsS_8 units shown propagating around the 2_1 axis along c . The triangular planes corresponding to the shared sulfurs are hatched to guide the viewing of the helix structure.

sulfurs pointing toward the $+c$ direction. The in-plane vs. out-of-plane $\text{Cs}-\text{S}$ distances are in the ranges of 3.43–3.74 Å and 3.61–3.87 Å, respectively. The averaged $\text{Cs}-\text{S}$ bond distance is 3.65 Å, comparable with the sum of Shannon radii, 3.53 Å, corresponding to the eight-coordinated Cs^+ (1.88 Å). The $\text{S}-\text{S}$ distances of the pentagonal edges range from 3.45 to 4.71 Å, much longer than 2.06 Å (twice the covalent radius).¹⁶

The CsS_8 polyhedra are arranged in a unique way in the van der Waals gap in that a fascinating helix framework similarly observed in the quartz structure is identified. As shown in Figure 4, the CsS_8 polyhedral units are all oriented in one direction and interconnected along the c axis through two shared sulfurs, $\text{S}(1)$ and $\text{S}(3)$, to form an extended helix propagating around the 2_1 screw axis. The formation of the helix can be recognized by viewing the alternation of the orientation of the hatched triangular planes associated with the shared sulfurs. The interchain interaction of parallel helices is extended along the plane of the van der Waals gap through sharing common sulfur atoms, $\text{S}(3)$ and $\text{S}(4)$.

One of the important aspects of this report is that the new compound adds an additional example to the collection of structurally related phases in the $\text{A}(\text{RE})\text{MQ}_4$ family (A = an alkali or alkaline-earth metal; RE = a rare-earth metal; M = a post-transition metal; Q = S , Se) for structural comparison. Through detailed structural analyses, the origin of the formation of a noncentrosymmetric lattice can be discerned. Chalcogenide compounds reported thus far in the $\text{A}(\text{RE})\text{MQ}_4$ family form three different but closely related layered-type structures, each of which can be represented respectively by one of the aforementioned chalcogenide phases, e.g., CsSmGeS_4 , KLaGeS_4 and CaYbInS_4 . These layered structures are characterized by the $[(\text{RE})\text{MS}_4]^{n-}$ ($n = 1, 2$) slabs that are stacked along one of the lattice dimensions with the A-site cations residing in between the slabs. The structural differences result from slight changes in the anion array and in turn the coordination geometries with

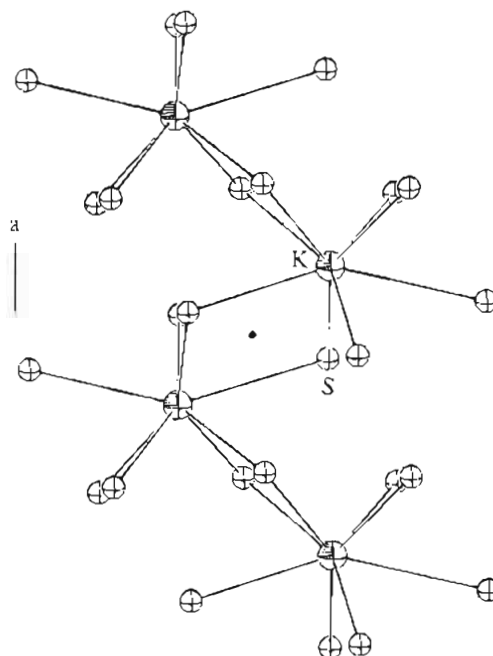


Figure 5. View of the interconnected KS_8 bicapped trigonal prism units. The solid dot represents the pseudo center of symmetry.

respect to the rare-earth cations and the A-site cations. Both the samarium and the lanthanum structures possess the same slab framework consisting of $(\text{RE})\text{S}_7$ mTPs and GeS_4 tetrahedra, whereas the ytterbium structure is composed of the $[\text{YbInS}_4]^{2-}$ slabs containing YbS_6 octahedra and InS_4 tetrahedra similar to that in the olivine structure. In addition, the CsSmGeS_4 and KLaGeS_4 structures are noncentrosymmetric with the space groups of $P2_12_12_1$ and $P2_1$, respectively, whereas the CaYbInS_4 structure is centrosymmetric with the space group $Pnma$.

The structural variations that correspond to the formation of noncentrosymmetric CsSmGeS_4 and KLaGeS_4 structures have been found interesting. In the KLaGeS_4 structure, the origin of the noncentrosymmetric lattice is reported to result from the distortion of the trigonal prisms that allows capping of an adjacent La atom by a sulfur atom. The distortion is such that the $\text{La}-\text{S}$ bond which arises from this capping sulfur is pointing in a unique direction throughout the entire unit cell. In comparison, although the slab structure remains identical in the title compound, the capping $\text{Sm}-\text{S}$ bonds of the neighboring slabs are pointing in opposite directions. As a result, the polar axes defined by the uniaxial $\text{Sm}-\text{S}$ bond interaction are alternating along the stacking direction of the $[\text{SmGeS}_4]^{2-}$ slabs due to the reversal of the capping direction and the unit cell length is doubled. It is interesting to note that, while an ordered reversal does not similarly happen in the KLaGeS_4 structure, the direction of the polar axis was indeterminable in bulk crystal due to racemic twinning during crystal formation.⁹ This difference in slab ordering is possibly induced by the preferred coordination geometries adopted by the KS_8 vs. CsS_8 polyhedra. In contrast to the preferential helical orientation observed in the extended CsS_8 chain, the KS_8 polyhedra can be essentially viewed as a chain of bicapped trigonal prisms (bTP), as shown in Figure 5, forming pairs related by a center of symmetry through shared edges of the polyhedra. The much different Ca^{2+} cation, smaller in size and double in charge compared with the Cs^+ and K^+ cations, is found in layers of ordered octahedral sites of the olivine-type CaYbInS_4 structure. This comparison renders the conclusion that the inclusion of large monovalent alkali metal cations likely yields the observed

(16) Cotton, F. A.; Wilkinson, G. *Advanced Inorganic Chemistry*, 5th ed.; John Wiley & Sons: New York, 1988.

noncentrosymmetric lattice. In the coordination compounds, such counterion effects have been observed previously.¹⁷

Conclusion

The novel layered mixed-metal CsSmGeS₄ phase represents another noncentrosymmetric phase of the A(RE)MQ₄ (1114) chalcogenide compounds family. An unusual helix structure made of CsS₈ units is identified, that is likely responsible for the formation of the noncentrosymmetric lattice. Comparison with two structurally related 1114 chalcogenides, KLaGeS₄ and CaYbInS₄ provides some insight for a possible route to the design synthesis of noncentrosymmetric compounds. The title

compound melts congruently at ~1086 °C and preliminary infrared absorption spectroscopy studies suggest that it is likely IR transparent. Growth of large-sized single crystals for detailed bulk optical property analysis is planned.

Acknowledgment. We gratefully acknowledge that this research has been supported by the Robert A. Welch Foundation. The authors are indebted to Mr. M. L. Pierson and Dr. J. C. Stormer, Jr., for microprobe analysis. Financial support for the single crystal X-ray diffractometer by the National Science Foundation is also acknowledged.

Supplementary Material Available: Text giving detailed synthetic procedures, a figure showing DTA curves, and tables of crystallographic data and anisotropic thermal parameters (4 pages). Ordering information is given on any current masthead page.

- (17) (a) Bernal, I.; Myrczek, J.; Cai, J. *Polyhedron* **1993**, *12*, 1149–1155.
(b) Bernal, I.; Cetrullo, J.; Myrczek, J.; Cai, J.; Jordan, W. *J. Chem. Soc., Dalton Trans.* **1993**, 1771–1776.